

Energy acceptance of the St. George recoil separator

Z. Meisel^{a,b,*}, M.T. Moran^b, G. Gilardy^{b,c}, J. Schmitt^{d,1}, C. Seymour^b, M. Couder^b

^a*Institute of Nuclear & Particle Physics, Department of Physics & Astronomy, Ohio University, Athens, OH 45701, USA*

^b*Department of Physics, Joint Institute for Nuclear Astrophysics, University of Notre Dame, Notre Dame, IN 46556, USA*

^c*Centre d'Études Nucléaires de Bordeaux Gradignan, UMR 5797 CNRS/IN2P3 - Université de Bordeaux, 19 Chemin du Solarium, CS 10120, F-33175 Gradignan, France*

^d*Department of Physics & Astronomy, Clemson University, Clemson, SC 29634, USA*

Abstract

Radiative alpha-capture, (α, γ) , reactions play a critical role in nucleosynthesis and nuclear energy generation in a variety of astrophysical environments. The St. George recoil separator at the University of Notre Dame's Nuclear Science Laboratory was developed to measure (α, γ) reactions in inverse kinematics via recoil detection in order to obtain nuclear reaction cross sections at the low energies of astrophysical interest, while avoiding the γ -background that plagues traditional measurement techniques. Due to the γ ray produced by the nuclear reaction at the target location, recoil nuclei are produced with a variety of energies and angles, all of which must be accepted by St. George in order to accurately determine the reaction cross section. We demonstrate the energy acceptance of the St. George recoil separator using primary beams of helium, hydrogen, neon, and oxygen, spanning the magnetic and electric rigidity phase space populated by recoils of anticipated (α, γ) reaction measurements. We find the performance of St. George meets the design specifications, demonstrating its suitability for (α, γ) reaction measurements of astrophysical interest.

Keywords:

Recoil mass separator; Radiative alpha-capture;

PACS: 26.20.Fj, 29.30.Aj

1. Introduction

Precise (α, γ) reaction cross sections are crucial to accurately model a variety of astrophysical phenomena [1], such as the production of the *s*-process neutron-source nucleus ^{22}Ne [2], the carbon-to-oxygen abundance ratio of stellar cores [3], nucleosynthesis in massive stars [4], the abundance of ^{44}Ti produced in core-collapse supernovae [5], and the nuclear reaction sequence occurring in type-I x-ray bursts [6]. Owing to the relatively low kinetic energies of nuclei in the relevant astrophysical conditions, traditional nuclear reaction measurements in which the outgoing γ ray is measured often suffer from prohibitively high γ -backgrounds and, for high *Q*-value reactions, complicated γ -ray cascades [7]. One approach which has been adopted to overcome this difficulty employs inverse kinematics and a recoil separator, in which the nuclear recoil produced in the (α, γ) reaction is electromagnetically separated from unreacted beam nuclei on the basis of their mass differences and identified with various combinations of time-of-flight and energy-loss measurements [8]. Recoil- γ coincidences substantially improve the signal-to-noise

compared to traditional techniques and provide significantly reduced cross section uncertainties [9].

In order to undertake (α, γ) reaction cross section studies at astrophysically relevant energies for nuclei with nuclear mass $A \leq 40$, the St. George recoil separator at the University of Notre Dame's Nuclear Science Laboratory (NSL) has been developed [10]. The recoil separator technique generally relies on using inverse kinematics, where a heavy ion beam is impinged on a lighter nuclear target; for (α, γ) reactions with St. George, the HIPPO helium gas-jet produces the desired target [11, 12]. Unreacted incident beam particles and nuclear reaction recoils both exit the gas-jet with similar momenta. For a typical cross section of $1 \mu\text{b}$ and a gas-jet density of 10^{17} atoms/cm², the ratio for recoils to unreacted beam nuclei is 1 part in 10^{13} . In order to be effective, a recoil separator must accept all (or most [13]) of the nuclear reaction recoils and have a mass separation sufficient to produce a recoil/beam ratio allowing for practicable particle identification.

Due to the prompt γ -ray emission, nuclear reaction recoils leave the target with a range of energies and angles, according to the reaction *Q*-value, γ -ray cascade, and γ emission angles [8]. For St. George, the 'acceptance' is the angle-energy phase space of nuclear reaction recoils that the separator transmits to the recoil detection-plane with 100% efficiency. Accurate cross section measurements with the recoil separator technique rely on a thorough charac-

*Corresponding author

Email addresses: meisel@ohio.edu (Z. Meisel), mcouder@nd.edu (M. Couder)

¹Present Address: Department of Physics and Astronomy, Michigan State University, East Lansing, MI 48824, USA

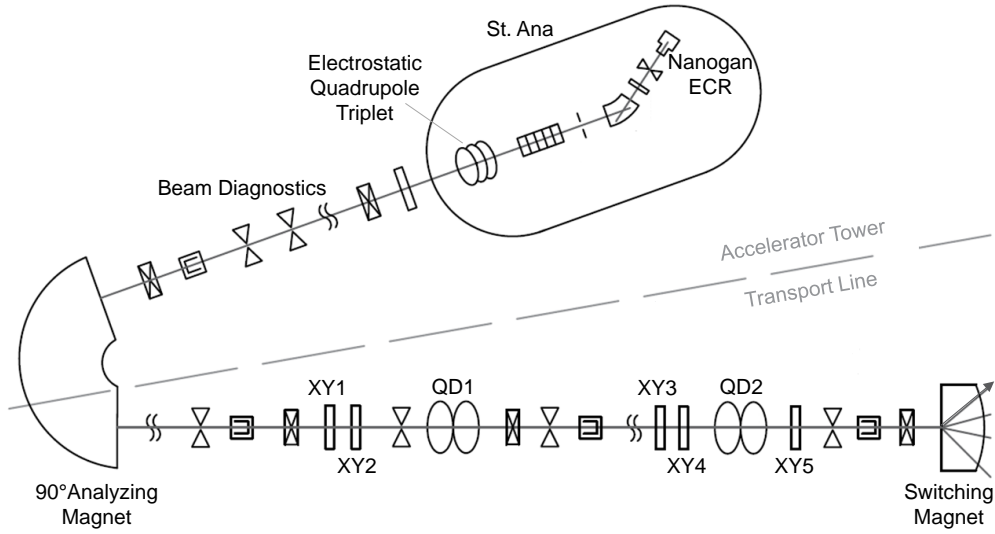


Figure 1: Schematic of the St. Ana accelerator and transport beam line to St. George (The vertical accelerator beam line is folded here for convenience.). “QD” correspond to quadrupole magnet doublets, which are used to focus the beam, while “XY” correspond to steerer magnets, which are used to ensure the beam is transported down the ion optical centers of the quadrupoles via small corrections.

terization of the recoil separator acceptance.

In a crucial first step of the St. George recoil separator commissioning process, we have determined the energy acceptance of St. George for a range of beam species, spanning the magnetic and electric rigidity phase space anticipated for recoils of future (α, γ) cross section measurements. We discuss the experimental set-up in Section 2, our energy acceptance measurement method in Section 3, and the measurement results and discussion thereof in Section 4, prior to summarizing our work in Section 5.

2. Experimental set-up

Stable ion beams are delivered to St. George by the recently installed 5 MV single-ended Pelletron accelerator St. Ana, from National Electrostatics Corporation², at the NSL. Ion beams produced by a Nanogan ECR ion source, from Pantechnik³, are accelerated with St. Ana, energy-selected by a 90° analyzing magnet, and transported down a ≈ 22 m beam-line, which contains several quadrupole and steerer magnets, to St. George with beam intensities upwards of 100 μA . The configuration of the transport line at the time of this experiment, shown in Figure 1, consisted of the horizontal X and vertical Y steerer magnet pair XY₁ and XY₂ following the accelerator momentum-analyzing magnet and preceding the quadrupole doublet QD₁, followed by said quadrupole doublet, steerer pair XY₃ and XY₄, the second quadrupole doublet QD₂, the single steerer XY₅, a dipole ‘switching’ magnet, and (not

shown) an XY steerer and a quadrupole triplet. Beam position monitors, Faraday cups, and fluorescing quartz windows are employed at various locations along the transport line to provide diagnostic information during beam tuning.

St. George consists of eighteen ion optical elements: six dipole magnets, eleven quadrupole magnets (four doublets and one triplet), and a Wien filter, as shown in Figure 2. The last quadrupole, Q11, is followed by an ion detection chamber in which ions can be identified via total energy loss and time-of-flight. Several ports are available along the St. George beam line and on the magnets for diagnostic equipment to assess the properties of transmitted ions. For future (α, γ) reaction measurements, St. George will be preceded by the HIPPO gas-jet [11], which will serve as a relatively uniform high-density reaction target [12]. For the acceptance measurements presented here, the primary beam from St. Ana was transmitted directly into St. George, where two 2 mm diameter collimators 20 cm apart were employed just prior to the entrance of St. George to ensure the beam entered St. George on-axis. The collimators had the added benefit of limiting beam currents to a few μA in order to protect diagnostic equipment.

Diagnostic equipment along St. George includes Faraday cups, fluorescing quartz windows, and electrically insulated slits. Faraday cups, used to monitor beam transmission, are located following the first, second, and fifth dipole magnets, the Wien filter, and the eleventh quadrupole magnet. Each Faraday cup is equipped with a -300 V secondary electron suppression electrode to ensure reliable current readings. Electrically insulated slits with current readouts, used for the energy acceptance measurements to monitor the beam width and centering, are located before

²<http://www.pelletron.com>

³<http://www.pantechnik.com>

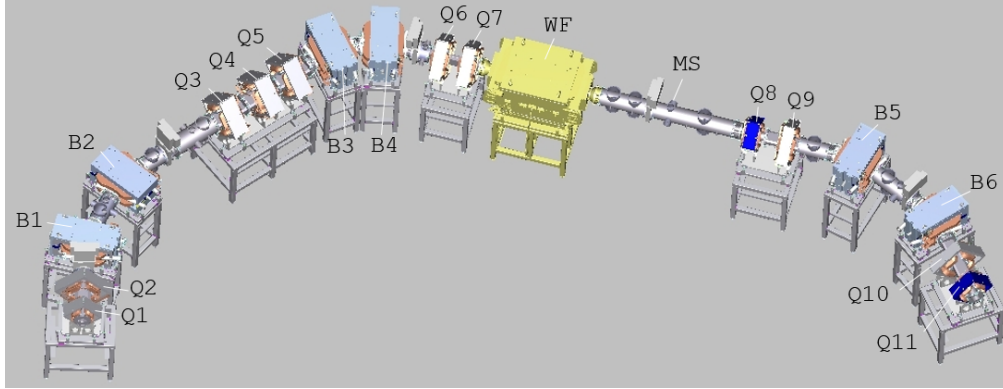


Figure 2: Schematic of the St. George recoil separator, where the labels correspond to “B” for dipole magnets, “Q” for quadrupole magnets, “WF” for the Wien filter, and “MS” for the mass slits. The target position is located upstream of Q1 and the recoil detection system (not shown) is downstream of Q11.

and after each dipole magnet, as well as 1.59 m downstream of the Wien filter exit. These slits will be used in future (α, γ) reaction measurements to improve beam-rejection properties of St. George. In particular, the slits following the Wien filter, referred to as the ‘mass slits’, are located at the position optimized for beam-rejection, which provides a horizontal achromatic focus for recoil nuclei. The slits and Faraday cups each have a lower-limit for their current sensitivity of ≈ 1 pA. The 0° exit port of the first, third, and fifth dipole magnets, as well as the exit port of the recoil detection chamber, are equipped with fluorescing quartz windows from McMaster-Carr⁴, outside of which (at atmosphere) is a camera. The quartz windows are used to assess the beam shape at their respective locations and, more importantly, are used to determine if the beam is being transported along the ion-optical center of the quadrupole magnets preceding that quartz. The quartz viewers also serve as a crude way to determine beam transmission, as their fluorescence is visible at relatively low beam currents.

3. Energy acceptance measurement method

In inverse kinematics, the products of an (α, γ) reaction are emitted from the target position with the same average momentum as the unreacted beam in a narrow cone, where the opening angle is primarily determined by the reaction Q -value and center-of-mass energy (See Equation 13 of Reference [8].). St. George is designed to accept and transmit all recoil nuclei of a single charge-state emitted from the target with a maximum angle of ± 40 mrad and energy spread from the central recoil energy of $\pm 8\%$ [10]. The maximum recoil energy deviations occur when γ rays are emitted at 0° or 180° in the center of mass.

In this study, we mimicked the recoil energy spread by employing a beam in the absence of a target in order to

verify that, at 0° (i.e. for no angular deflection), 100% of ions within $\pm 8\%$ of the energy for which the separator was tuned were transmitted to the end of St. George. A similar technique was employed to determine the energy acceptance of the ERNA recoil separator [14, 15]. Transmission through the recoil separator was determined by comparing beam current measurements provided by the Faraday cups at the target location and in the recoil detection plane, where equal currents correspond to 100% transmission. Various charge states and beam energies were employed for ions of helium, hydrogen, neon, and oxygen in order to determine the energy acceptance for nuclei within the designed electric and magnetic rigidity⁵ limits of St. George, $E\rho \leq 5.7$ MV and $0.1 \text{ Tm} \leq B\rho \leq 0.45 \text{ Tm}$, respectively [10].

The energy acceptance measurements for each species, defined by a given $B\rho$ – $E\rho$, consisted of two main procedures, which each consisted of several steps. Summarized briefly, the first procedure consisted of adjusting the magnetic elements prior to and within St. George to ensure that the ion beam was traveling down the ion optical center of the separator when at the tune-energy. The second procedure consisted of adjusting the focusing elements within St. George to maximize the energy range about the tune-energy within which all ions would be transmitted through the separator. The second procedure was necessary to find the optimal tune about the nominal ion optical settings [10] provided by calculations performed with the software COSY Infinity⁶ [16].

The first procedure, centering the ion beam within St. George so that quadrupole magnets only provided focusing and not beam steering, was accomplished by performing the following steps:

⁵For an ion of kinetic energy T in MeV, mass A in MeV, and charge q in units of the electron charge, $B\rho = \frac{\sqrt{T^2 + 2TA}}{300q} \text{ Tm}$ and $E\rho = \frac{2T}{q} \text{ MV}$.

⁶<http://www.bt.pa.msu.edu/index.cosy.htm>

⁴<http://www.mcmaster.com>

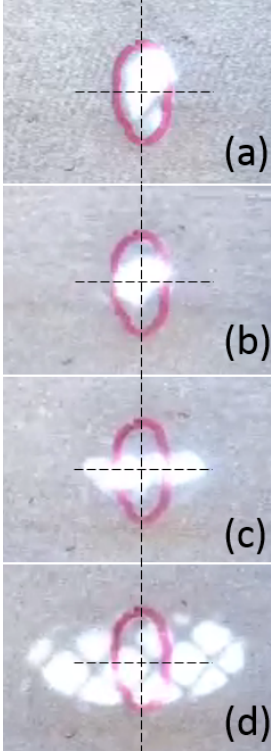


Figure 3: Demonstration of a non-steering ion optical tune. (a)-(d) show images of the B3 dipole magnet 0° quartz viewer for a 1 MeV H^+ beam, where the Q2 quadrupole magnet is scaled from its minimum field strength (a) up to ≈ 0.13 T, which is $\sim 50\%$ of its maximum value (d), where (b) and (c) are at arbitrary intermediate field strengths. The red oval and black crosses provide a reference for the size and center of the beam. The height and width of the red oval correspond to ≈ 3 mm and ≈ 1.5 mm, respectively, on the quartz viewer.

- 1.1. The accelerator magnetic and electrostatic elements and St. Ana transport beam-line magnetic elements (See Figure 1.) were adjusted to deliver an ion beam of the chosen species and energy with a current of several hundred nA to the St. George target location. The accelerator and transport line elements were adjusted to send beam through the two collimators at the target location.
- 1.2. With no field in the B1 dipole magnet⁷, the beam was impinged on the B1 0° quartz viewer. The Q1 and Q2 quadrupole magnets of St. George separately had their field strengths adjusted from the minimum to $> 50\%$ of the maximum field strength. The image of the beam-spot on the B1 0° exit-port fluorescing-quartz was monitored for shifts in the spot centroid. Any deviation from a ‘non-steering’ beam, shown in Figure 3, was corrected by adjusting the last few steering magnets of the St. Ana transport line.

⁷We note that residual magnetic fields on the dipoles do not impact our methods, as the effect would only be a horizontal translation of the beam spot on a quartz viewer.

- 1.3. The B1 and B2 dipole magnets were adjusted to their nominal fields for the species of interest at the tune-energy, sending the beam to the B3 0° exit-port quartz-viewer, with no field on the B3 dipole. The correction process of the previous step was repeated. Though this step is seemingly redundant, the longer distance of travel of the beam from Q1 and Q2 to this quartz provided a higher sensitivity to the presence of steering in the ion optics. This step could not be repeated for the 0° exit port of the B5 dipole magnet since the ion beam was too defocused at that location without using quadrupole magnets Q3–Q9, a necessary condition to test for beam steering.
- 1.4. With fields on Q1 and Q2 set to provide a narrow waist at the B3 0° exit-port quartz-viewer, the B1 and B2 fields were adjusted to minimize steering in the quadrupole magnets Q3–Q5. These adjustments were generally within $\lesssim 0.3\%$ of the calculated optimal field setting. A tune with simultaneously non-steering Q1–Q2 and Q3–Q5 was not achievable, likely due to a minor misalignment of the quadrupole magnets. However, the shift of the beam spot position from steering was minimized to a vertical deflection of $\lesssim 2.5$ mm on the quartz viewer, which corresponds to a maximum deflection of $\lesssim 2$ mrad by the Q5 quadrupole magnet at maximum field strength. Given the Q5 field gradient, the observed deflection indicates the vertical misalignment of the Q3–Q5 quadrupoles is $\lesssim 1$ mm with respect to the Q1–Q2.
- 1.5. Quadrupole magnets Q1–Q5 and dipole magnets B3–B4 were adjusted to their nominal fields for the species of interest at the tune-energy, sending the beam to the B5 0° exit-port quartz-viewer, with no field on the B5 dipole. A small electric field was applied to the Wien filter to offset the residual magnetic field. The B3 and B4 fields were adjusted to achieve the non-steering condition on the B5 0° exit-port quartz-viewer for the Q6–Q7 quadrupole magnets.
- 1.6. The Wien filter magnetic and electric fields, as well as the magnetic field clamps, were set to their nominal values for the species of interest at the tune-energy. The Wien filter magnetic field was then adjusted to achieve the non-steering condition for the Q8–Q9 quadrupole magnets on the B5 0° exit-port quartz-viewer.
- 1.7. The electrically insulated slits with charge readouts located 1.59 m downstream of the Wien filter, the so-called ‘mass slits’, were then closed to the point of reading $\lesssim 1$ pA on the left and right mass slits. This provides a measurement of the beam width, which we can use to estimate the anticipated beam-rejection of the separator.
- 1.8. The B5 and B6 dipole magnets were then set to and adjusted about their nominal field settings for the

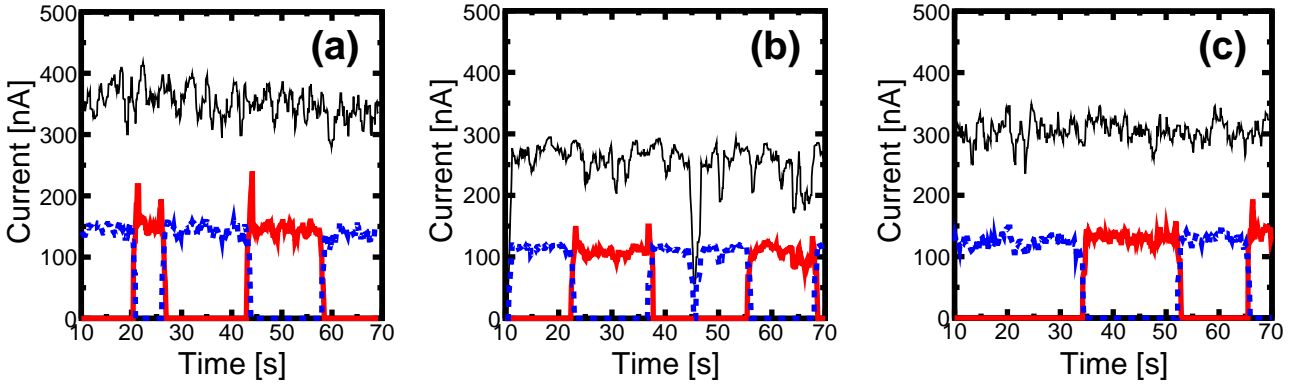


Figure 4: (color online.) Demonstration of 100% beam transmission through St. George for $^{16}\text{O}^{2+}$ ions with the recoil separator tuned for $B\rho = 0.421\text{ Tm}$, $E\rho = 2.0\text{ MV}$ (2 MeV ions, in this case.). Figures (a), (b), and (c) show the beam current read at the target location (thick red lines), detector plane (thick blue-dashed lines), and collimator upstream of St. George used to monitor the incoming beam-current stability (thin black lines), for 2 MeV (a), 2.16 MeV (b), and 1.84 MeV (c) ions.

species of interest at the tune-energy until the non-steering condition was achieved for the quadrupole magnets Q10–Q11 on the quartz-viewer located on the 0° exit port of the recoil detection chamber.

The second procedure, maximizing the energy acceptance of St. George, was accomplished by performing the following steps:

- 2.1. Transmission was checked by monitoring the beam current on a collimator upstream of the target location and monitoring the beam current on Faraday cups at the target and recoil detection locations, while extending and retracting the target location Faraday cup (See Figure 4.). For the calculated ion optical tune for the species of interest, we did not find 100% beam transmission from the target location to the recoil detector plane. Therefore, the quadrupole magnets Q1–Q11 required adjustment to achieve 100% transmission. With all other quadrupole magnets set to their nominal field setting, each quadrupole was individually adjusted in order to maximize the beam transmission to the recoil detector plane. Then, for each of the N quadrupole magnets which improved beam transmission upon adjustment, the field was adjusted from the nominally calculated value by $1/N$ times the individual adjustment required for that quadrupole magnet to improve beam transmission. This naïve scaling procedure resulted in 100% beam transmission (See Figure 4a.).
- 2.2. Having achieved 100% beam transmission for the tune-energy, the St. Ana terminal voltage was adjusted so that the beam would have an energy -8% below the tune-energy, e.g. to 1.84 MeV from a tune-energy of 2 MeV. In general, 100% transmission was not achieved. If beam current was lost on

the mass slits, quadrupole magnets Q1–Q6 were adjusted as described in the previous step to optimize beam transmission. Once beam current was removed from the mass slits, quadrupole magnets Q8–Q11 were adjusted as described in the previous step to optimize beam transmission.

- 2.3. Beam transmission was checked again with the accelerator adjusted back to the tune-energy. If 100% beam transmission was not achieved, the procedure from the previous step was repeated. This and the previous step were performed iteratively until 100% beam transmission was obtained for both the tune-energy and the $-8\% \frac{\Delta E}{E}$ energy.
- 2.4. Having achieved 100% transmission for the tune-energy and -8% below the tune-energy, the St. Ana terminal voltage was adjusted so that the beam would have an energy +8% above the tune-energy, e.g. to 2.16 MeV from a tune-energy of 2 MeV. If 100% transmission was not achieved, adjustments needed to be made to Q1–Q11. These adjustments, along with a re-verification of transmission at the tune-energy and -8% below the tune-energy, were performed in an iterative fashion, as described in the previous step. In general, we found the ion optical tune needed little to no adjustment to achieve 100% transmission at +8% above the tune-energy once 100% transmission was achieved for the tune-energy and -8% below the tune-energy.

We note that the second of the two aforementioned procedures was greatly expedited for ensuing energy acceptance measurements, as the suspected optimum values for the nominal tune were improved with time. For instance, for the third successful energy acceptance measurement only a single adjustment of quadrupole magnets Q10–Q11 was required in order to achieve $\pm 8\%$ energy

acceptance.

Figure 4 demonstrates $\pm 8\%$ energy-acceptance for a 2 MeV $^{16}\text{O}^{2+}$ beam. The fluctuations observed in beam intensity are thought to be mainly due to instabilities in the St. Ana ECR ion source. The spikes in current for the Faraday cup at the target location following its insertion and retraction are thought to be due to current induced by the motion of the cup apparatus.

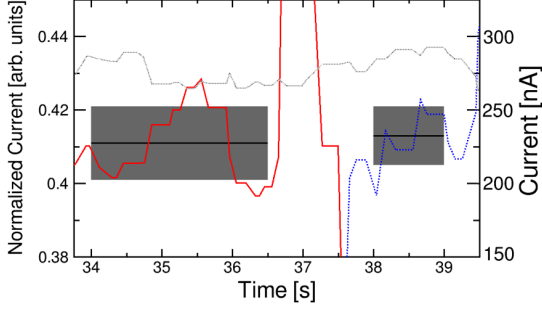


Figure 5: (color online.) Demonstration of $>99\%$ beam transmission through St. George for 2.16 MeV $^{16}\text{O}^{2+}$ ions with the recoil separator tuned for $B\rho = 0.421$ Tm, $E\rho = 2.0$ MV (2 MeV ions, in this case.). The ratio (left axis) of the current on the target-cup (red line) and detector cup (blue-dashed line) to the upstream collimator current are shown for a time of near-constant upstream collimator current (gray-dotted line, right axis). Two gray boxes indicate (1) horizontally: the time-frame during which the target cup is not moving, in order to avoid unwanted current induced by the motion of the cup and (2) vertically: the average current ratio (black line) and standard deviation of the current ratio (gray band). The mean current ratios differ by less than 1%, indicating better than 99% beam transmission.

As seen in Figure 5, we observe full transmission to a precision of ~ 1 nA for a beam intensity of ~ 100 nA, i.e. $> 99\%$.

4. Results and Discussion

Energy acceptance measurements were performed as described in the previous section for 8 ion beams, which were chosen to span the phase space of $E\rho$ and $B\rho$ where recoil nuclei from (α, γ) reactions of astrophysical interest are anticipated. Table 1 lists the ion beams for which an energy acceptance measurement was performed.

The field strengths for the ion-optical elements of St. George which were used for the energy acceptance measurements generally agreed with the values provided by the calculations featured in Reference [10]. However, the absence of an angular opening of the beam for the energy acceptance measurements performed here allowed for considerable flexibility in the ion optical tune of St. George. We expect the full angular and energy acceptance measurements performed in the future to provide much tighter constraints on the settings of the ion-optical elements.

We compare the magnetic rigidity of measured ions to recoils of astrophysical interest in Figure 6. Our measurements verify the required energy acceptance for the major-

Table 1: Ion beams for which $\pm 8\%$ energy acceptance was verified for the St. George recoil separator. Uncertainties for kinetic energy T , magnetic rigidity $B\rho$, and electric rigidity $E\rho$ are $\approx 1\%$, which is dominated by the present uncertainty of the analyzing magnet energy calibration.

| Species | Mass [u] | Charge [e] | T [MeV] | $B\rho$ [Tm] | $E\rho$ [MV] |
|-----------------------|----------|------------|-----------|--------------|--------------|
| $^{16}\text{O}^{4+}$ | 16 | 4 | 2.0 | 0.211 | 1.0 |
| $^1\text{H}^{1+}$ | 1 | 1 | 1.0 | 0.149 | 2.0 |
| $^4\text{He}^{1+}$ | 4 | 1 | 1.0 | 0.298 | 2.0 |
| $^{20}\text{Ne}^{4+}$ | 20 | 4 | 4.0 | 0.333 | 2.0 |
| $^{16}\text{O}^{2+}$ | 16 | 2 | 2.0 | 0.421 | 2.0 |
| $^4\text{He}^{2+}$ | 4 | 2 | 3.0 | 0.258 | 3.0 |
| $^{16}\text{O}^{4+}$ | 16 | 4 | 6.0 | 0.365 | 3.0 |
| $^{16}\text{O}^{4+}$ | 16 | 4 | 8.0 | 0.421 | 4.0 |

ity of the range of astrophysical interest, where example cases considered for the design of St. George (See Table 1 of Reference [10].) are chosen for comparison. We show only the low $E\rho$ cases highlighted in Reference [10], since the high $E\rho$ cases are in general less astrophysically interesting due to the corresponding high kinetic energies that are absent in all but the highest temperature environments. Our acceptance measurements also demonstrate the capability to, for instance, repeat the $^3\text{He}(\alpha, \gamma)^7\text{Be}$ measurement performed with the recoil separator ERNA [18]. Such a measurement may help to improve constraints on Big Bang nucleosynthesis [6] and resolve discrepancies in solar fusion calculations [20], particularly if performed in conjunction with angle-resolved γ -detection at the target location. Furthermore, a direct measurement of $^{22}\text{Ne}(\alpha, \gamma)^{26}\text{Mg}$ in the energy range previously studied in regular kinematics [19] is well within reach, which would help constrain the role of the $^{22}\text{Ne}(\alpha, n)$ s -process neutron source. Finally, we demonstrate our ability to accept ^{16}O recoils from $^{12}\text{C}(\alpha, \gamma)$, noting that the large angular acceptance anticipated for St. George will allow the lowest-energy direct measurement of this reaction to date.

We used the measured width of the beam at the mass slits, as determined in Step 1.7, to provide a first-order estimate of the anticipated beam rejection capabilities of St. George. The smallest anticipated spatial separation between beam and recoil nuclei provided by the Wien filter is ≈ 5 cm, which is for the case of an (α, γ) reaction on an $A = 40$ nucleus. In order to achieve the desired mass rejection of 1 part in 10^{15} , the magnitudes of the beam and recoil nuclei distributions must be similar at the location of the mass slits when the amplitude of the beam distribution is 10^{15} times larger than the amplitude of the recoil distribution. If we assume beam and recoil nuclei both have Gaussian horizontal distributions with the same width, but the beam distribution is 10^{15} larger in amplitude and has a centroid 5 cm horizontally displaced from the recoil distribution centroid, a standard deviation

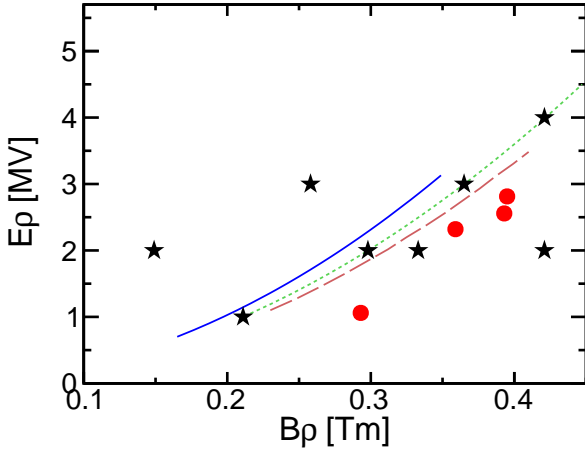


Figure 6: (color online.) Rigidity phase space designed to be accepted by the St. George recoil separator, where the $B\rho$ - $E\rho$ of ions with a measured energy acceptance are indicated with black stars. Examples of recoils of astrophysical interest, low recoil-energy cases from Table 1 of Reference [10], assuming the most populous equilibrium charge-state from the dilute gas model of Reference [17] that is within the $B\rho$ - $E\rho$ limits of St. George, are indicated by the red-filled circles. The solid blue line indicates the $B\rho$ - $E\rho$ space for $q = 2^+$ recoils from the ${}^3\text{He}(\alpha, \gamma){}^7\text{Be}$ reaction at the energies measured in the past with the recoil separator ERNA [18]. The long-dashed mauve line corresponds to ${}^{26}\text{Mg}^{6+}$ recoils from the ${}^{22}\text{Ne}(\alpha, \gamma)$ reaction for energies covered by a previous measurement in forward kinematics [19]. The short-dashed green line corresponds to ${}^{16}\text{O}^{4+}$ recoils from ${}^{12}\text{C}(\alpha, \gamma)$ for center of mass energies from 700–3000 keV.

of $\sigma \approx 4$ mm for both distributions is sufficient to achieve a 1:1 ratio of beam-to-recoil nuclei -3σ left of the beam-line center at the mass slits (3σ is chosen as the point for comparison since $\pm 3\sigma$ encompasses 99.8% of the recoil distribution.). In Step 1.7 we determined the width of the ion distribution at the mass slits is $w \leq 20$ mm, which corresponds to intercepting $\lesssim 1$ pA out of the full ~ 100 nA ion intensity (i.e. $\sim 0.001\%$). For a Gaussian distribution, this implies a mass slit opening of $\pm 4.5\sigma$. Therefore, from our measurement of w , we deduce $\sigma \lesssim 2.2$ mm, which is far less than the 4 mm required for the desired mass rejection. We note that our estimate is a best-case scenario since more pathological beam distributions are often observed⁸. Furthermore, this estimate neglects effects such as beam scattering within the separator which adversely impact the mass rejection.

5. Conclusions

We present first results from commissioning of the St. George recoil separator. By performing measurements of stable ion beams of varied elements, charge-states, and energies,

we verify that St. George meets the design specifications of providing an energy acceptance of $\pm 8\%$ within the separator's rigidity phase space. Our ultimately employed magnetic field strengths generally agree with predictions from ion-optical calculations performed with COSY Infinity; however, some deviations persist. We attribute present disagreements to the absence of realistic field maps in the calculations and an absence of an angular opening of the beam at the target location, which will be more restrictive when determining the optimum ion-optical tune. Our comparison to the properties of recoils from anticipated future nuclear reaction measurements demonstrates that St. George will be a vital tool used to obtain precise cross sections for (α, γ) reactions of astrophysical interest.

Acknowledgements

We thank the staff of the Nuclear Science Laboratory at the University of Notre Dame for their outstanding support. This material is based upon work supported by the National Science Foundation under Grants No. 1062819, 1419765, and 1430152, and the Nuclear Regulatory Commission under Grant No. NRC-HQ-12-G-38-0073.

References

- [1] C. R. Brune, B. Davids, Ann. Rev. Nucl. Part. S. 65 (2015) 87.
- [2] F. Käppeler, et al., Astrophys. J. 437 (1994) 396.
- [3] M. Wiescher, F. Käppeler, K. Langanke, Annu. Rev. Astron. Astr. 50 (2012) 165.
- [4] C. Tur, A. Heger, S. Austin, Astrophys. J. 671 (2007) 821.
- [5] G. Magkotsios, F. X. Timmes, A. L. Hungerford, C. L. Fryer, P. A. Young, M. Wiescher, Astrophys. J. Suppl. S. 191 (2010) 66.
- [6] R. H. Cyburt, A. M. Amthor, A. Heger, E. Johnson, Z. Meisel, H. Schatz, K. Smith, Astrophys. J. 830 (2016) 55.
- [7] A. Cacioli, et al., Eur. Phys. J. A 39 (2009) 179.
- [8] C. Ruiz, U. Greife, U. Hager, Eur. Phys. J. A 50 (2014) 99.
- [9] C. Akers, et al., Phys. Rev. Lett. 110 (2013) 262502.
- [10] M. Couder, G. Berg, J. Görres, P. LeBlanc, L. Lamm, E. Stech, M. Wiescher, J. Hinnfeld, Nucl. Instrum. Meth. A 587 (2008) 35.
- [11] A. Kontos, et al., Nucl. Instrum. Meth. A 664 (2012) 272.
- [12] Z. Meisel, K. Shi, A. Jemcov, M. Couder, Nucl. Instrum. Meth. A 828 (2016) 8.
- [13] C. Matei, et al., Phys. Rev. Lett. 97 (2006) 242503.
- [14] D. Rogalla, et al., Nucl. Instrum. Meth. A 513 (2003) 573.
- [15] D. Rogalla, et al., Eur. Phys. J. A 6 (1999) 471.
- [16] K. Makino, M. Berz, Nucl. Instrum. Meth. A 427 (1999) 338.
- [17] R. O. Sayer, Rev. Phys. Appl. 12 (1977) 1543.
- [18] A. Di Leva, et al., Phys. Rev. Lett. 102 (2009) 232502.
- [19] K. Wolke, et al., Z. Phys. A 334 (1989) 491.
- [20] E. G. Adelberger, et al., Rev. Mod. Phys. 83 (2011) 195.

⁸This has been observed by an in-beam fluorescing quartz viewer located after the mass slits, which was added to the set-up following the measurements described in this work.